Application of Large Pore MCM-41 Molecular Sieves To Improve Pore Size Analysis Using Nitrogen Adsorption Measurements

M. Kruk and M. Jaroniec*

Department of Chemistry, Kent State University, Kent, Ohio 44242

A. Sayari

Department of Chemical Engineering and CERPIC, Université Laval, Ste-Foy, Quebec, Canada G1K 7P4

Received July 11, 1997. In Final Form: September 5, 1997[⊗]

MCM-41 siliceous molecular sieves were used to test the applicability of the Kelvin equation for nitrogen adsorption in cylindrical pores of the size from 2 to 6.5 nm. It was shown that the Kelvin equation for the hemispherical meniscus, corrected for the statistical film thickness, is in quite good agreement with an experimental relation between the pore size and the capillary condensation pressure. The agreement can be made quantitative in the pore size range from ca. 2 to 6.5 nm, if a simple correction to the Kelvin equation is introduced. The required statistical film thickness curve (*t*-curve) was calculated using nitrogen adsorption data for large pore MCM-41 samples and the obtained results were extrapolated using an adsorption isotherm for a macroporous silica gel. Moreover, an accurate analytical representation of the *t*-curve was found. Since both the corrected Kelvin equation for cylindrical pores and the *t*-curve have simple analytical forms, they can conveniently be used in a variety of methods to evaluate porosity. It was shown that the BJH method with the corrected Kelvin equation accurately reproduces pore sizes of MCM-41 materials. A comparison was made between the specific surface areas for the MCM-41 samples calculated on the basis of the BET equation and those obtained using other independent methods. The results strongly suggest that when nitrogen adsorption data are used, the BET method overestimates the specific surface area of siliceous materials. The latter conclusion was supported by the examination of the obtained statistical film thickness curve.

Introduction

An evaluation of the specific surface area and the pore size is a fundamental problem in gas adsorption[1,2] and has been a subject of numerous experimental and theoretical studies (see refs 1, 3, and 4 and references therein). A milestone in the assessment of the specific surface area was the development of the Brunauer−Emmett−Teller (BET) method,[5] which has become a standard tool for surface area estimation.[1,2] As far as the pore size assessment is concerned, a variety of methods were proposed and extensively applied.[1] Many of them are based on the Kelvin equation,[1,2] which relates the pore size with the pressure of the capillary condensation or evaporation. It was soon recognized that the formation of the adsorbed film on pore walls plays an important role in adsorption processes in porous media and the pore radius obtained from the Kelvin equation represents the radius of the pore space confined by the adsorbed film. Therefore, a correction for the statistical film thickness has to be introduced into the Kelvin equation to yield the actual pore size.[1] The latter idea was very effectively implemented in the Barrett−Joyner−Halenda (BJH) method[6] to calculate pore size distributions under the assumption of a cylindrical shape of pores.

For many years, a direct experimental verification of adsorption methods to evaluate surface area and porosity was exceptionally difficult due to the lack of well-defined high surface area porous or nonporous solids. In principle, other experimental techniques can be used for verification purposes, but actually their accuracy can be expected to be rather inferior to that of gas adsorption methods. Recently, computer simulations and other theoretical approaches were applied to test the applicability of the Kelvin equation (see ref 7 and references therein) and it was suggested that the latter equation underestimates the pore sizes in the range up to ca. 7.5 nm, even when it is corrected for the statistical film thickness.

The discovery of ordered mesoporous M41S materials[8,9] opened new opportunities in evaluating the surface area and porosity. For the first time, well-defined mesoporous solids of a simple pore geometry,[8−11] tailored pore size,[8−20] reproducible surface properties,[18,20,21] and different

* E-mail: Jaroniec@kentvm.kent.edu. Phone: (330) 672 3790. Fax: (330) 672 3816.

⊗ Abstract published in *Advance ACS Abstracts,* October 15, 1997.

(1) Gregg, S. J.; Sing, K. S. W. *Adsorption, Surface Area and Porosity*; Academic Press: London, 1982.

(2) Sing, K. S. W.; Everett, D. H.; Haul, R. A. W.; Moscou, L.; Pierotti, R. A.; Rouquerol, J.; Siemieniewska, T. *Pure Appl. Chem.* **1985**, *57*, 603-619.

(3) Jaroniec, M.; Madey, R. *Physical Adsorption on Heterogeneous Solids*; Elsevier: Amsterdam, 1988.

(4) Rudzinski, W.; Everett, D. H. *Adsorption of Gases on Heterogeneous Solid Surfaces*; Academic Press: London, 1991.

(5) Brunauer, S.; Emmett, P. H.; Teller, E. *J. Am. Chem. Soc.* **1938**, *60*, 309−319.

(6) Barrett, E. P.; Joyner, L. G.; Halenda, P. P. *J. Am. Chem. Soc.* **1951**, *73*, 373−380.

(7) Lastoskie, C.; Gubbins, K. E.; Quirke, N. *J. Phys. Chem.* **1993**, *97*, 4786−4796.

(8) Kresge, C. T.; Leonowicz, M. E.; Roth, W. J.; Vartuli, J. C.; Beck, J. S. *Nature* **1992**, *359*, 710−712.

(9) Beck, J. S.; Vartuli, J. C.; Roth, W. J.; Leonowicz, M. E.; Kresge, C. T.; Schmitt, K. D.; Chu, C. T-W.; Olson, D. H.; Sheppard, E. W.; McCullen, S. B.; Higgins, J. B.; Schlenker, J. L. *J. Am. Chem. Soc.* **1992**, *114*, 10834−10843.

(10) Huo, Q.; Margolese, D. I.; Ciesla, U.; Feng, P.; Gier, T. E.; Sieger, P.; Leon, R.; Petroff, P. M.; Shüth, F.; Stucky, G. D. *Chem. Mater.* **1994**, *6*, 1176−1191.

(11) Chen, C.-Y.; Li, H.-X.; Davis, M. E. *Microporous Mater.* **1993**, *2*, 17−26.

(12) Sayari, A., *Chem. Mater.* **1996**, *8*, 1840−1852.

(13) Sayari, A. In *Recent Advances and New Horizons in Zeolite Science and Technology*, Chon, H., Woo, S. I., Park, S.-E., Eds.; Elsevier: Amsterdam, 1996; pp 1-46.

S0743-7463(97)00776-2 CCC: $14.00

compositions[12−14] became available. The MCM-41 molecular sieve, which is a member of the M41S family, exhibits a hexagonal arrangement of uniform cylindrical pores and is especially suitable as a model adsorbent.[20,22,24]

In our previous study,[20] a relation between the pressure of nitrogen condensation in ordered mesopores and their pore diameters was reported, but the range of pore sizes used (2−3.8 nm) was too narrow to develop a meaningful analytical expression for such a relation. Recently, a series of samples structurally similar to MCM-41 was used by Naono et al.[19] to obtain a relation between the pressure of nitrogen condensation and the pore size. Moreover, the nitrogen statistical film thickness curve was assessed for relative pressures between 0.13 and 0.44. The obtained data were used in the BJH method to obtain a better estimate of the pore size distributions in the range of pore diameters from 2 to 4 nm. Although the work of Naono et al. was interesting and inspiring, several crucial points need to be further explored. Firstly, the method of the pore size evaluation for model samples can be improved. Secondly, the obtained statistical film thickness curve and the relation between the pore size and the capillary condensation pressure were limited to the relative pressure range from ca. 0.13 to 0.44, and no analytical form was provided, which would make the reported data much more useful for practical applications.

In the current study, a more reliable method of the pore size evaluation was used. Moreover, the pore diameter range exhibited by our model samples was much broader (2−6.5 nm), since in addition to MCM-41 silicates prepared via a conventional method using surfactants of different alkyl chain lengths,[20] large pore materials were obtained via postsynthesis hydrothermal treatment.[18] A new method to calculate the statistical film thickness was developed and shown to provide consistent results for a series of large pore samples. The obtained *t*-curves were extrapolated using nitrogen adsorption data for a macroporous silica gel to obtain the statistical film thickness curve valid in a relative pressure range from 10^{-5} to 0.985 with a very accurate analytical representation by the Harkins−Jura equation. Subsequently, a modified Kelvin equation was proposed in order to quantitatively reproduce the experimental relation between the pore size and capillary condensation pressure for cylindrical pores. The latter equation can conveniently be used to calculate mesopore size distributions and is not restricted to the pore size range of our model adsorbents. Finally, the accuracy of the BET method was critically examined against our model experimental data.

Experimental Section

Materials. The synthesis procedure for large pore MCM-41 materials was described elsewhere.[15,18] The samples obtained in a conventional manner in the presence of cetyltrimethylammonium bromide were subjected to a postsynthesis hydrothermal treatment in their mother liquor at 423 K under static conditions for required periods of time (from 19 h to 3 days). The treatment led to a gradual pore size increase, resulting in materials in the pore size range from 3.5 to 6.5 nm. In addition, MCM-41 samples of smaller pore diameters (from ca. 2 to 4 nm) were synthesized using alkyltrimethylammonium bromide surfactants with alkyl chain lengths of 8, 10, 12, 14, and 16 carbon atoms. The procedure was reported elsewhere.[20]

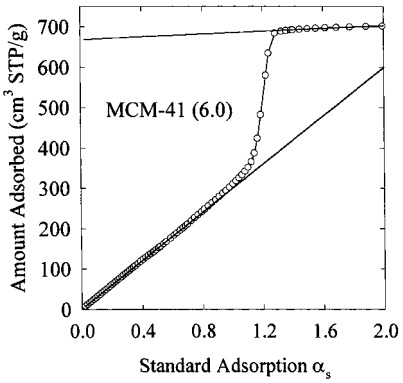

Figure 1. High-resolution α_s-plot for the MCM-41 (6.0) sample.

The samples are denoted as MCM-41 (*w*), where *w* is the pore diameter (in nanometers) for a given sample, calculated using X-ray diffraction spacing d_{100} (later denoted as *d*) and primary mesopore volume, as described below. Macroporous silica gels LiChrospher Si-1000 (S_{BET} = 25 m^2/g) and LiChrospher Si-4000 (S_{BET} = 10 m^2/g) used as reference adsorbents were acquired from EM Separations (Gibbstown, NJ).

Measurements. X-ray diffraction (XRD) spectra were obtained on a Siemens D5000 diffractometer using nickel-filtered Kα radiation. Nitrogen adsorption−desorption measurements were carried out on an ASAP 2010 volumetric adsorption analyzer from Micromeritics (Norcross, GA). Before the measurements, the samples of MCM-41 silicates were outgassed in the degas port of the adsorption apparatus.

Calculations. The total surface area S_t, external surface area S_{ex}, and primary mesopore volume V_p of the samples were calculated using the high-resolution α_s-plot method.[1,18,25] The α_s-plot method is based on a comparison of the adsorption isotherm for a given porous material with adsorption data for a reference macroporous solid. Note that according to the IUPAC recommendations,[2] pores are classified as micropores (width w below 2 nm), mesopores (2 nm < *w* < 50 nm), and macropores (*w* > 50 nm). Moreover, in the current work, uniform cylindrical pores of MCM-41 materials are referred to as primary mesopores, while other mesopores present are designated as secondary mesopores. The external surface area is defined as the surface area of macropores and secondary mesopores. In the α_s-plot calculations, a macroporous silica gel LiChrospher Si-1000 (S_{BET} = 25 m^2/g) was used as a reference adsorbent.

The primary mesopore volume V_p and external surface area S_{ex} were calculated from the slope of a linear portion of the α_s-plot in the pressure range above the pressure of nitrogen condensation in primary mesopores, but below the onset of capillary condensation in secondary mesopores (see Figure 1). In most cases, the relative pressure intervals from 0.45 to 0.85 and from 0.75 to 0.92 (i.e., standard reduced adsorption α_s range from 1.05 to 1.7 and from 1.4 to 2) were used for small pore and large pore samples, respectively. Note that the standard reduced adsorption is defined as $\alpha_s = v_{ref}(p/p_0)/v_{ref}(0.4)$, where $v_{ref}(p/p_0)$ and $v_{ref}(0.4)$ are the amount adsorbed for the reference solid as a function of relative pressure and the amount adsorbed at the relative pressure of 0.4, respectively. The total surface area S_t was calculated from the slope of the initial part of the α_s-plot, i.e., for relative pressures below 0.1 (α_s below 0.7). For most samples, the initial portion of the plot was linear and passed through the origin of the graph (see Figure 1). In the case of the MCM-41 (2.0), (2.8), (5.8), and (6.5) samples, the line drawn through the linear part of the α_s-plot intersected the "amount adsorbed" axis slightly above its origin. Such a behavior for the

(14) Raman, N. K.; Anderson, M. T.; Brinker, C. J. *Chem. Mater.* **1996**, *8*, 1682−1701.
(15) Khushalani, D.; Kuperman, A.; Ozin, G. A.; Tanaka, K.; Garces, J.; Olken, J. J.; Coombs, N. *Adv. Mater.* **1995**, *7*, 842−846.
(16) Huo, Q.; Margolese, D. I.; Stucky, G. D. *Chem. Mater.* **1996**, *8*, 1147−1160.
(17) Ulagappan, N.; Rao, C. N. R. *Chem. Commun.* **1996**, 2759−2760.
(18) Sayari, A.; Liu, P., Kruk, M.; Jaroniec, M. *Chem. Mater.*, in press.
(19) Naono, H.; Hakuman, M.; Shiono, T. *J. Colloid Interface Sci.* **1997**, *186*, 360−368.
(20) Kruk, M.; Jaroniec, M.; Sayari, A. *J. Phys. Chem. B* **1997**, *101*, 583−589.
(21) Kruk, M.; Jaroniec, M.; Sayari, A. *Microporous Mater.* **1997**, *9*, 173−182.
(22) Branton, P. J.; Hall, P. G.; Sing, K. S. W. *J. Chem. Soc., Chem. Commun.* **1993**, 1257−1258.
(23) Franke, O.; Schulz-Ekloff, G.; Rathousky, J.; Starek, J.; Zukal, A. *J. Chem. Soc., Chem. Commun.* **1993**, 724−726.
(24) Ravikovitch, P. I.; Domhnaill, S. C. O.; Neimark, A. V.; Schüth, F.; Unger, K. K. *Langmuir* **1995**, *11*, 4765−4772.
(25) Kaneko, K.; Ishii, C.; Ruike, M.; Kuwabara, H. *Carbon* **1992**, *30*, 1075−1088.

MCM-41 (5.8) and (6.5) samples arises most likely from the presence of small amounts of micropores, as discussed elsewhere,[18] but in two other cases, it results probably from increased gas−solid interactions due to significant curvature of pore walls of these small pore samples.[20] The BET surface area S_{BET} of the reference adsorbent is used in the α_s-plot calculations of the total surface area, and therefore the latter method provides another, more convenient way of obtaining S_{BET}. The advantage of the α_s-plot method arises from the fact that the calculations are not restricted to the adsorption data in a conventional BET relative pressure range (ca. 0.05−0.3). In such a pressure range, the condensation in primary mesopores (or for large pore samples, the enhancement of adsorption in the latter pores before the condensation takes place) may lead to a significant overestimation of the specific surface area using the standard BET method.[20] However, adsorption isotherm data for relative pressures below ca. 0.1 can conveniently be utilized in the α_s-plot calculations to avoid the use of higher pressure data strongly biased by the condensation in primary mesopores. Note that the surface area of primary mesopores S_p can be calculated as the difference between the total surface area S_t and the external surface area S_{ex}.

The size of primary mesopores w_d for the MCM-41 samples was calculated on the basis of the following formula:[18,20,21,26]

$$w_d = cd\left(\frac{\rho V_p}{1 + \rho V_p}\right)^{1/2} \quad (1)$$

where d is the (100) interplanar spacing obtained from XRD, ρ is the density of walls of the samples ($\rho = 2.2$ g/cm^3),[26,27] and $c = (8/(3^{1/2}\pi))^{1/2} = 1.213$ is a constant. Equation 1 was derived for the infinite structure of uniform cylindrical pores of the size w_d arranged in a hexagonal pattern with the (100) interplanar spacing d and therefore is applicable for MCM-41 molecular sieves. Since the distance between pore centers a is easily available from the interplanar spacing d ($a = 2/3^{1/2}d$), one can evaluate the pore wall thickness b_d as the difference between a and the pore diameter w_d. The primary mesopore size w_d and volume V_p were used to estimate the specific surface area of primary mesopores (denoted here as S_d):

$$S_d = \frac{4V_p}{w_d} \quad (2)$$

Equation 2 is analogous to the formula to calculate the diameter of cylindrical pores on the basis of their volume and surface area: $w_{4V/S} = 4V/S$. The latter equation was extensively used in studies of MCM-41 materials[19,23] and critically compared with other methods of the pore size evaluation.[20,28]

The statistical film thickness of nitrogen adsorbate on the pore walls of MCM-41 materials (as a function of relative pressure p/p_0) was estimated from the ratio of the adsorbed amount in primary mesopores to their maximum adsorption capacity:

$$t(p/p_0) = \frac{w_d}{2}\left[1 - \left(\frac{v_{p,\,max} - v_p(p/p_0)}{v_{p,\,max}}\right)^{1/2}\right] \quad (3)$$

where $v_p(p/p_0)$ is the amount adsorbed in primary mesopores as a function of pressure and $v_{p,\,max}$ is the maximum adsorption capacity of primary mesopores. The former was assessed from the adsorption isotherm $v(p/p_0)$ for a given sample by subtracting the amount adsorbed on its external surface:

$$v_p(p/p_0) = v(p/p_0) - \frac{S_{ex}}{S_{BET,\,ref}} v_{ref}(p/p_0) \quad (4)$$

In equation 4, $S_{BET,\,ref}$ and $v_{ref}(p/p_0)$ are the BET specific surface area and the adsorption isotherm, respectively, for the reference adsorbent used in calculations of the external surface area S_{ex}. The maximum amount adsorbed, $v_{p,\,max}$ was set to be equal to the adsorption at the relative pressure of 0.85 ($v_{p,\,max} = v_p(0.85)$). At such a pressure, the primary mesopores of the MCM-41 materials used in the current study can be assumed to be completely filled with nitrogen, but yet the pressure is below the onset of capillary condensation in secondary mesopores. The occurrence of the latter phenomenon would make eq 4 inaccurate, since the course of adsorption on the external surface area would no longer be satisfactorily described by the isotherm of the reference macroporous solid. Note that the validity of eq 3 rests upon an assumption that the density of the adsorbed film on the pore walls is equal to the density of the adsorbate after the pore is completely filled.

The pore size distributions were calculated using the Barrett−Joyner−Halenda (BJH) method.[6] The BJH method was also used to assess the specific surface areas S_{BJH} of the samples under study. Detailed information about the statistical film thickness curve and the modified Kelvin equation used is provided in the Results.

Table 1. Structural Parameters of the MCM-41 Samples under Study[a]

sample	d (nm)	w_d (nm)	V_p (cm^3/g)	S_{ex} (m^2/g)	S_t (m^2/g)	S_d (m^2/g)	S_{BJH} (m^2/g)
(2.0) [C8][b]	2.83	2.04	0.25	120	660	480	580
(2.8) [C10][b]	3.05	2.78	0.58	60	1040	840	950
(3.1) [C12][b]	3.34	3.13	0.67	90	1070	860	980
(3.3) [C14][b]	3.39	3.26	0.78	40	1120	950	1040
(3.8) [C16][b]	3.87	3.84	0.92	180	1180	960	1100
(4.1)	4.29	4.11	0.76	40	920	740	810
(4.6) [TR2-25h][c]	4.69	4.62	0.88	30	960	760	860
(5.5) [TR3-24h][c]	5.52	5.53	0.97	40	860	700	750
(5.8) [TR1-3d][c]	6.59	5.77	0.50[d]	80	470[d]	340	440
(6.0)	5.89	5.96	1.04	50	860	700	750
(6.2)	6.40	6.24	0.83	50	680	530	580
(6.5) [TR1-2d][c]	6.59	6.53	0.91[d]	60	720[d]	740	810

[a] d = XRD (100) interplanar spacing; w_d = primary mesopore size calculated using eq 1; V_p = primary mesopore volume; S_{ex} = external surface area; S_t = total surface area; S_d = surface area of primary mesopores calculated from V_p and w_d; S_{BJH} = surface area calculated using the BJH method with the modified Kelvin equation (eq 9). [b,c] References 20 and 18, respectively, where the samples were described in detail (symbols of the samples used in the references are provided in square brackets). [d] Data were corrected for the presence of microporosity.[18]

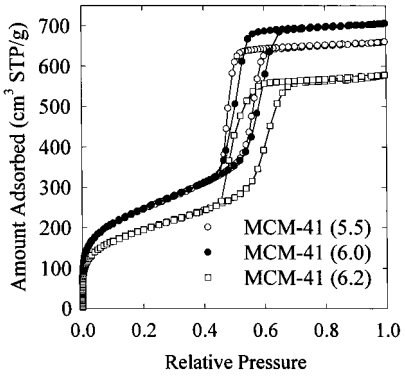

Figure 2. Nitrogen adsorption isotherms for MCM-41 samples used to calculate the statistical film thickness curve.

Results

The (100) interplanar spacing d, primary mesopore diameter w_d, total surface area S_t, primary mesopore volume V_p, and external surface area S_{ex} for the samples are listed in Table 1. It needs to be noted that V_p, S_{ex}, and w_d values for the MCM-41 (2.0)−(3.8) materials are slightly different than those reported earlier,[20] due to a more reliable reference adsorption isotherm used in the current study. Nitrogen adsorption isotherms for selected large pore MCM-41 samples are shown in Figures 2 and 3. It can be noticed that the adsorption−desorption process is not reversible, which manifests itself in the presence of more or less pronounced hysteresis loops in contrast to

(26) Dabadie, T.; Ayral, A.; Guizard, C.; Cot, L.; Lacan, P. *J. Mater. Chem.* **1996**, *6*, 1789−1794.
(27) Marler, B.; Oberhagemann, U.; Vortmann, S.; Gies, H. *Microporous Mater.* **1996**, *6*, 375−383.
(28) Maddox, M. W.; Olivier, J. P.; Gubbins, K. E. *Langmuir* **1997**, *13*, 1737−1745.

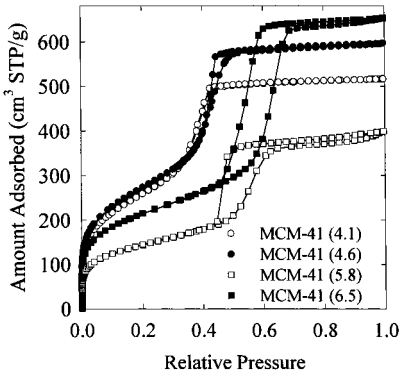

Figure 3. Nitrogen adsorption isotherms for selected MCM-41 samples.

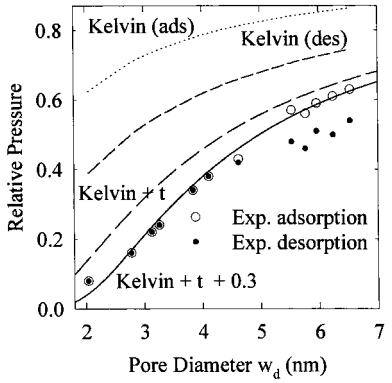

Figure 4. Comparison of the experimentally obtained relation between the pore size and the pressure of capillary condensation (hollow circles) and capillary evaporation (filled circles) with (i) the Kelvin eq 6 for adsorption in cylindrical pores (denoted on the graph as Kelvin (ads)), (ii) the Kelvin eq 7 for desorption in cylindrical pores (Kelvin (des)), (iii) the Kelvin eq 7 with a correction for the statistical film thickness eq 8 (Kelvin + *t*), and (iv) the modified Kelvin equation corrected for the statistical film thickness, eq 9 (Kelvin + *t* + 0.3).

the nitrogen adsorption behavior of the MCM-41 samples with smaller pores, where reversibility was observed.[20,22,23] One can attempt to find correlations between positions of inflection points on adsorption and desorption branches of the isotherms and the pore size w_d of the materials. As can be seen in Figure 4, it is possible to obtain a useful and unambiguous relation between the pressure of capillary condensation and the pore size. However, it is much more difficult to find such a correlation for desorption (capillary evaporation) because of the following two reasons. Firstly, the isotherms are reversible up to the relative pressure of about 0.40. In the case of samples for which the condensation in primary mesopores takes place slightly above the latter pressure limit, the irreversibility can be observed, but the adsorption and desorption branches are not parallel to each other. Instead, the desorption branches decline abruptly for relative pressures close to 0.4−0.45 and the resulting hysteresis loops are triangular in shape (see Figure 3) and their breadths are highly dependent upon the position of the adsorption branch. As a result, the pore size range of about 4−5.5 nm corresponds to a rather narrow interval of capillary evaporation pressures (see Figure 4). Moreover, for samples with pores larger than ca. 5 nm, the width of the hysteresis loop is dependent on the quality of a given sample, since for less uniform materials, i.e., MCM-41 (5.8) and (6.2), the hysteresis loops are relatively broad (see Figure 2 and 3). As can be seen in Figure 4, differences in quality between the samples seem to considerably affect the relation between the capillary evaporation (desorption) pressure and the pore size, making it somewhat ambiguous, but their impact on adsorption (capillary condensation) behavior is much smaller.

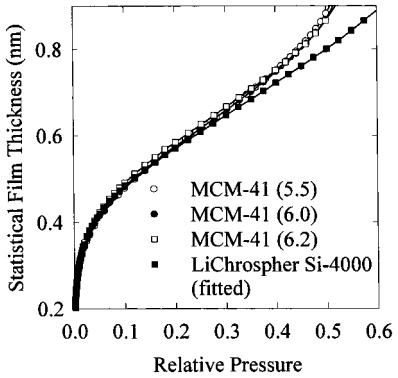

Figure 5. Statistical film thickness curves obtained from eq 3 and their fit with the adsorption isotherm for macroporous silica gel LiChrospher Si-4000.

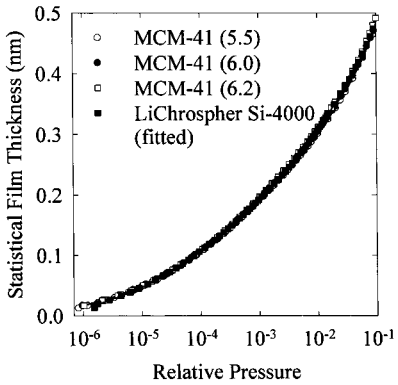

Figure 6. Statistical film thickness curves obtained from eq 3 for the low-pressure range and their fit with the adsorption isotherm for macroporous silica gel LiChrospher Si-4000.

Adsorption isotherm data shown in Figure 2 for three large pore MCM-41 molecular sieves were used to obtain the statistical film thickness of nitrogen adsorbed on the pore walls. Equation 3 was applied in the calculations. The resulting statistical film thickness curves (later referred to as *t*-curves) are shown in Figures 5 and 6. They are in excellent agreement with each other up to the relative pressure of ca. 0.5, for which the capillary condensation in primary mesopores of the samples starts to take place. Moreover, the *t*-curves are similar to the statistical film thickness data reported recently.[19] The obtained *t*-curves can be used in the BJH or similar methods of the pore size calculation, but they cover a limited range of pressures. However, it is desirable to have a reliable statistical film thickness curve valid for much higher pressures. Therefore, the adsorption isotherm for a macroporous silica gel LiChrospher Si-4000 was fitted to the experimental *t*-curves, as can be seen in Figures 5 and 6. One can notice that the fitted *t*-curve is in remarkably good agreement with the data calculated through eq 3 up to the relative pressure of at least 0.3. Moreover, higher pressure *t*-curve data for the MCM-41 samples under study may already be obscured by the enhancement of adsorption before the onset of capillary condensation, which may be the reason of differences between those *t*-curves and the fitted *t*-curve for the macroporous silica gel. It was found that the obtained film thickness curve $t(p/p_0)$ can be accurately represented in the relative pressure range from 0.1 to 0.95 by the Harkins−Jura equation of the following form:

$$t(p/p_0) = 0.1\left[\frac{60.65}{0.03071 - \log(p/p_0)}\right]^{0.3968} \qquad (5)$$

where t is expressed in nanometers. It needs to be noted that LiChrospher Si-4000 does not show appreciable evidence of capillary condensation up to ca. $0.985p/p_0$. Therefore, it can represent the t-curve for pressures higher than those for our reference adsorbent LiChrospher Si-1000 used for the α_s-plot method (ca. $0.96p/p_0$). The statistical film thickness curve obtained from fitting the isotherm data for LiChrospher Si-4000 was used in our BJH calculations.

Shown in Figure 4 is the comparison of our experimental relation between the pore size and the pressure of capillary condensation and capillary evaporation with various forms of the Kelvin equation. In the case of capillary condensation in cylindrical pores, the meniscus of the adsorbate was often assumed to be cylindrical (see ref 1 and references therein), which led to the following form of the Kelvin equation:

$$r(p/p_0) = \frac{\gamma V_L}{RT \ln[(p_0/p)]} \quad (6)$$

where V_L is the molar volume of the liquid adsorbate, γ is its surface tension, R is the universal gas constant, and T is the absolute temperature. In the current study, the data from ref 19 were used ($\gamma = 8.88 \times 10^{-3}$ N/m, $V_L = 34.68$ cm^3/mol, and $R = 8.314$ J/(mol·K)) and the measurements were performed at the liquid nitrogen temperature (77 K).

During the desorption process, the meniscus of the condensed adsorbate was usually assumed to be hemispherical and the following form of the Kelvin equation was obtained:[1]

$$r(p/p_0) = \frac{2\gamma V_L}{RT \ln[(p_0/p)]} \quad (7)$$

It was recognized (see refs 1 and 6 and references therein) that the Kelvin equation provides the so-called core radius instead of the actual pore radius. The core radius is the radius of the inner free space in the pore, which is not yet filled with the adsorbate during adsorption at a particular pressure, or the radius of the space in the pore, which will be emptied by the capillary evaporation during desorption. Therefore, in order to obtain the actual pore radius, the Kelvin equation needs to be corrected for the statistical film thickness on the pore walls (the corrected form of the equation for the hemispherical meniscus is shown below):

$$r(p/p_0) = \frac{2\gamma V_L}{RT \ln[(p_0/p)]} + t(p/p_0) \quad (8)$$

As expected, it can be seen in Figure 4 that eqs 6 and 7 do not provide an adequate representation of the relation between the capillary condensation (or evaporation) pressure and the pore radius. After the correction for the statistical film thickness is introduced, the Kelvin equation for the hemispherical meniscus (eq 8) was found to be in quite good agreement with the experimental data for adsorption (capillary condensation) in pores of the MCM-41 materials. It occurred that the application of eq 8 led to an underestimation of the pore radii of the samples under current study by about 0.3 nm. Therefore, the following corrected form of the Kelvin equation was used in our calculations of pore size distributions by means of the BJH method:

$$r(p/p_0) = \frac{2\gamma V_L}{RT \ln[(p_0/p)]} + t(p/p_0) + 0.3 \text{ nm} \quad (9)$$

As can be seen in Figure 4, eq 9 provides an excellent representation of our experimental relation between the pore size and the pressure of capillary condensation. It needs to be noted that a similar correction to the Kelvin equation has already been proposed by others.[29]

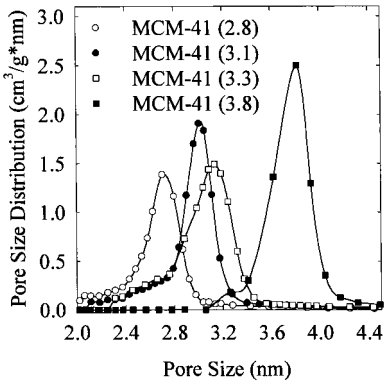

Figure 7. BJH pore size distributions for selected MCM-41 samples.

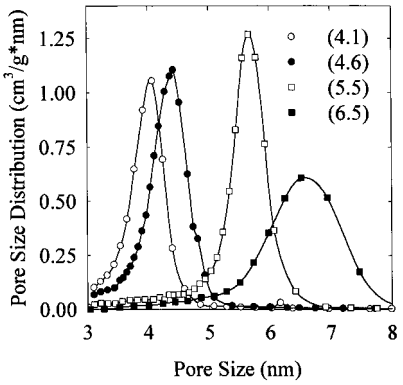

Figure 8. BJH pore size distributions for selected MCM-41 samples including large pore MCM-41 (5.5) and (6.5) molecular sieves.

Shown in Figures 7 and 8 are pore size distributions calculated from adsorption data using the BJH method with the corrected Kelvin equation (eq 9) and the experimental film thickness curve (which can be satisfactorily approximated by eq 5). One can notice that maxima of the pore size distributions for MCM-41 molecular sieves are in quantitative agreement (usually within 0.1 nm) with the pore sizes of the materials, calculated through eq 1. Listed in Table 1 are specific surface areas S_{BJH} for the samples obtained from the BJH method (using eq 9) and surface areas of primary mesopores S_d obtained from geometrical considerations (eq 2). The sum of S_d and the external surface area S_{ex} for a given sample provides an estimate of its specific surface area, as does S_{BJH} and the total surface area S_t calculated from the α_s-plot method. It occurred that $S_d + S_{ex}$ is usually much closer to S_{BJH} than to S_t and the ratio $(S_d + S_{ex})/S_t$ or S_{BJH}/S_t is about 0.9 for most of the samples.

Discussion

The Kelvin equation for the cylindrical shape of the meniscus (eq 6) was supposed to be valid for adsorption, whereas the Kelvin equation for the hemispherical meniscus (eq 7) was assumed to describe the course of desorption in cylindrical pores (see ref 1 and references therein). The present study strongly indicates that in the case of nitrogen at 77 K, eq 7 is actually applicable for

(29) Maglara, E.; Kaminski, R.; Conner, W. C. In *Characterization of Porous Solids IV*; McEnaney, B., Mays, T. J., Rouquerol, J., Rodrigues-Reinoso, F., Sing, K. S. W., Unger, K. K.; Royal Society of Chemistry: London, 1997; p 25.

adsorption, rather than desorption. Moreover, in order to qualitatively reproduce the relation between the pore size and the capillary condensation pressure, the correction for the statistical film thickness (eq 8) needs to be introduced. The current study suggests that the agreement can be made quantitative in the pore size range from ca. 2 to 6.5 nm, when the radius obtained from the Kelvin equation for a hemispherical meniscus is incremented by 0.3 nm. The obtained relation between the pore size and the capillary condensation pressure (eq 9) is in excellent agreement with recent nonlocal density functional[24] and computer simulation studies.[28] Since the modified Kelvin equation has a simple analytical form (eq 9), it can conveniently be used to calculate pore size distributions from nitrogen adsorption data for various materials with pore sizes from ca. 2 to 100 nm. However, further studies will be needed to assess the actual range of validity of the equation and its applicability for pore shapes other than cylindrical and materials of different surface properties than porous silicas. It also needs to be noted that it is not clear what form of the Kelvin equation would be applicable for pore size calculations on the basis of nitrogen desorption at 77 K, since the usually applied form (eq 8) appears to be significantly inaccurate (see Figure 4), at least in the pore diameter range from 2 to 6.5 nm.

It was observed that widths of hysteresis loops are highly dependent on the quality of the samples. As can be seen in Figures 2 and 3, some large pore samples, such as MCM-41 (5.5) or (6.0), have relatively narrow hysteresis loops, whereas for others, e.g., MCM-41 (5.8) and (6.2), the hysteresis loops are considerably broadened. The observed broadening of hysteresis loops most likely arises from lack of uniformity of pore diameter along cylindrical pores of the materials. During desorption, narrower pore parts, which still contain condensed nitrogen, may prevent the capillary evaporation from wider parts of the pores.[30,31] A similar effect was recently studied using computer simulations[32] and shown to considerably lower the pressure of capillary evaporation in pores with narrow constrictions. Pore connectivity effects may be an additional cause of the observed broadening of hysteresis loops, since the large pore samples were obtained by the hydrothermal restructuring process,[15,18] which may lead to a degradation of the pore structure of the materials. It was shown by transmission electron microscopy[15] that in the course of the hydrothermal treatment, pores of the MCM-41 samples became less regular and some pore walls seemed to be broken or missing. Low-pressure nitrogen adsorption data[18] provide strong evidence of a gradual development of microporosity, when the thermal restructurization was carried out for extended periods of time. It was suggested that holes in broken walls of the materials act as micropores with respect to nitrogen molecules. In the case of MCM-41 (5.8), the α_s-plot analysis indicated the presence of a small amount of micropores,[18] so some effect of connectivity of cylindrical pores of the material cannot be precluded. However, there was no evidence of degradation of the porous structure for MCM-41 (6.2) and the broadening of its hysteresis loop is most probably solely due to single pore effects caused by considerable variations of the diameter along the cylindrical pores of the material.

It was recognized[30,31] that the pore connectivity affects only desorption branches of isotherms. This hypothesis is consistent with the data presented in Figure 4, since the experimental relation between the pore size and the capillary condensation pressure is smooth within experimental error and does not seem to be much affected by the quality of the samples. Contrarily, the relation between the capillary evaporation pressure and the pore size above ca. 4 nm is somewhat ambiguous. In principle, one can ignore data for lower quality samples and use the remaining data to establish an unambiguous relation, but this does not seem to be useful from the point of view of practical applications. The samples usually studied are expected to have pore shapes much less defined than our lower quality model materials, and therefore the relation between the capillary evaporation pressure and the pore size, obtained on the basis of high-quality samples, would be primarily of theoretical interest.

It also needs to be noted that although nitrogen adsorption is a standard and most commonly used method of evaluating surface area and porosity,[1,2] the adsorption−desorption behavior of nitrogen at 77 K in the pore size range explored in our experimental study is quite exceptional, since the isotherms are reversible for pores of the size up to about 4 nm.[20,22,23] For other adsorbates,[33,34] such as argon or oxygen, there are marked hysteresis loops for samples with pores of sizes well below 4 nm. In such cases, the relation between the pore size and the pressure of the capillary evaporation would probably not exhibit peculiarities observed for nitrogen desorption at relative pressures ca. 0.4−0.45 and therefore would be potentially useful in the pore size range considered in the current study (from 2 to 6.5 nm). However, the effects of pore shape nonuniformity (or, more generally, pore connectivity) are likely to make the latter relation somewhat ambiguous in a similar way, as was already discussed above for nitrogen adsorption−desorption data.

The experimental data reported in the current study allow for an assessment of the specific surface area from the BJH method (S_{BJH}) or geometrical considerations (S_d calculated using eq 2). These two methods are independent of the standard BET method, which underlies the evaluation of the total surface area S_t using the high-resolution α_s-plot, since the BET specific surface area[1,18] of the reference adsorbent is used in the calculations. Therefore, comparison of the results of different methods to evaluate the specific surface area provides a test of reliability of the BET method in studies of silica gels. The latter are known to have strongly heterogeneous surfaces,[28,35−37] which may make the BET model (localized multilayer adsorption without lateral interactions on homogeneous surfaces) inaccurate. As already discussed by others,[28] the BET surface area for materials with uniform cylindrical pores, such as MCM-41, approximately corresponds to the area of cylinders passing through the centers of adsorbed molecules forming the monolayer on the surface, rather than to the actual surface area of the material. This would result in an underestimation of the surface area by the factor of about $(w - \sigma_m)/w$, where w is the diameter of the pore and it is assumed that the adsorbed molecules are spheres of a diameter σ_m. However, when results of our surface area calculations based on the BET method (S_t) were compared with other estimations of the specific surface area, it occurs that the former were 10−15 % higher than the latter, in contrast

(30) Liu, H.; Zhang, L.; Seaton, N. A. *J. Colloid Interface Sci.* **1993**, *156*, 285−293.
(31) Ball, P. C.; Evans, R. *Langmuir* **1989**, *5*, 714-723.
(32) Maddox, M. W.; Lastoskie, C. M.; Quirke, N.; Gubbins, K. E. In *Fundamentals in Adsorption*; LeVan, M. D., Ed.; Kluwer: Boston, 1996; pp 571−578.
(33) Branton, P. J.; Hall, P. G.; Sing, K. S. W.; Reichter, H.; Schuth, F.; Unger, K. K. *J. Chem. Soc., Faraday Trans.* **1994**, *90*, 2965−2967.
(34) Llewellyn, P. L.; Grillet, Y.; Schuth, F.; Reichter, H.; Unger, K. K. *Microporous Mater.* **1994**, *3*, 345.
(35) *The Colloidal Chemistry of Silica*; Bergna, H. E., Ed.; American Chemical Society: Washington, DC, 1994.
(36) Bereznitski, Y.; Jaroniec, M.; Kruk, M.; Buszewski, B. *J. Liq. Chromatogr.* **1996**, *19*, 2767.
(37) Kruk, M.; Jaroniec, M.; Gilpin, R. K.; Zhou, Y. W. *Langmuir* **1997**, *13*, 545−550.

to what could be expected on the basis of considerations presented above. To explain the observed behavior, it is helpful to examine the statistical film thickness curve obtained on the basis of our experimental data. It can be seen in Figure 5 that the statistical film thickness is about 0.47 nm for the relative pressure value of 0.09, which in the case of silicas usually corresponds to a surface coverage of one monolayer according to the BET method. The obtained statistical monolayer film thickness is considerably higher than those assumed in previous studies. For example, de Boer and co-workers[38] used the value of 0.354 nm in their studies. Therefore, it is very likely that actually the statistical monolayer coverage of nitrogen molecules on the surface of porous silicas (silica gels, siliceous MCM-41) is attained at pressures much lower than ca. 0.09 (which is obtained from the BET calculations). As a result, the actual monolayer capacity and, consequently, the specific surface area for siliceous adsorbents would also be lower than those calculated on the basis of the standard BET method. This would improve an agreement with the surface area estimations obtained using the BJH method and geometrical considerations (eq 2). The suggested overestimation of the specific surface area for silicas by the BET method may result from a strong surface heterogeneity of these adsorbents. Their surfaces feature different silanol and siloxane groups,[35] which exhibit a broad range of interaction energies with respect to nitrogen adsorbate molecules.[18,28,36,37] It is remarkable that low pressure nitrogen adsorption isotherms for siliceous materials are smooth to such an extent that no evidence of distinct monolayer formation step can be noticed,[20,36,37] in contrast to low-pressure adsorption data for many other adsorbents, for example, nongraphitized carbon blacks.[39] Such a behavior clearly shows that the formation of the first adsorbed layer strongly overlaps with the multilayer formation, which may be the reason for a significant inaccuracy of the BET model. The conclusions about the overestimation of the surface area of silicas by the BET method using nitrogen adsorbate are preliminary, and further studies are needed to fully understand the reported surface phenomena and their influence on calculations of the specific surface area.

Conclusions

MCM-41 mesoporous molecular sieves are convenient model adsorbents and provide a unique opportunity of testing fundamental adsorption methods to evaluate porosity and surface area. Until recently, such model studies were much more difficult to perform due to lack of good quality MCM-41 samples of pore sizes above ca. 4.5 nm. This problem was overcome using hydrothermal restructuring of MCM-41 samples synthesized in a conventional manner, which allows us to obtain good quality materials with pore diameters up to at least 6.5 nm. In the current study, MCM-41 samples of pore sizes in the range from 2 to 6.5 nm were used to test the applicability of different forms of the Kelvin equation to predict the relation between the pore size and the pressure of nitrogen capillary condensation/evaporation. It was shown that the Kelvin equation for a hemispherical meniscus (eq 7) with a correction for the statistical film thickness can quantitatively reproduce our experimental nitrogen adsorption (capillary condensation) data. The agreement can be made quantitative in the pore diameter range from ca. 2 to 6.5 nm, when the obtained pore radius values are incremented by 0.3 nm (eq 9). It occurred that it would be difficult to find a useful relation between the pressure of capillary evaporation and the pore size in this pore size interval because of the following two reasons. Firstly, the nitrogen adsorption−desorption isotherms are reversible up to the relative pressure of about 0.4. The isotherm curves for materials with pores of the size between ca. 4 and 5 nm, for which the capillary condensation takes place for relative pressures higher than but still close to 0.4, exhibit triangular hysteresis loops. A shift of the position of the desorption branch of the isotherm with a pore size increase is much smaller than the corresponding shift of the adsorption branch. This makes the readings of the pore size from the position of the desorption branch more prone to experimental error of the pressure evaluation. Secondly, for larger pore samples, which have a hysteresis loop with two parallel branches, the position of the desorption branch depends not only on the pore size but also on the quality of the samples. Samples of lower uniformity have their hysteresis loops considerably broadened, which can be explained as an effect of considerable variations of pore diameter along cylindrical pores of these model materials. In the course of desorption, narrower pore parts, which still contain condensed nitrogen, can be expected to hinder the capillary evaporation from wider pore parts, which do not have a direct access to the gas phase, causing "single pore" blocking effects. The fact that the position of the adsorption branch of the isotherm is not appreciably affected by the quality of samples is in agreement with previous reports suggesting that pore blocking effects are operative only during desorption.

The modified Kelvin equation for cylindrical pores and the statistical film thickness curve obtained in the current study were successfully used in the BJH pore size calculations for MCM-41 materials in the pore size range from 2 to 6.5 nm. Moreover, the reported equations are expected to be very useful in studies of various siliceous materials. The BJH method was shown to allow us to monitor very subtle structural changes in modified mesoporous silicas.[37] Therefore, the attained improvement of the pore size evaluation is likely to make the BJH method particularly useful in studies of mesoporous siliceous materials.

The comparison of specific surface area values estimated on the basis of the standard BET method (using the high-resolution α_s-plot) with other estimates of the surface area suggests that the BET method significantly overestimates the specific surface area of siliceous adsorbents, such as silica gels or MCM-41. Such a behavior results probably from the high heterogeneity of the silica surface, which causes a considerable overlap of the monolayer formation with multilayer adsorption. The examination of the *t*-curve obtained in the current study suggests that the statistical monolayer film thickness is attained for pressures significantly below those predicted on the basis of the BET monolayer capacity for a given sample. This would indicate that the monolayer capacity and, consequently, the specific surface area are actually lower than those obtained on the basis of the standard BET method. Further studies are needed to verify these conclusions about the surface area estimation for porous silicas.

Acknowledgment. The authors thank P. Liu for assistance in preparation of large pore MCM-41 samples.

LA970776M

(38) Lippens, B. C.; Linsen, B. G.; de Boer, J. H. *J. Catalysis* **1964**, *3*, 32.

(39) Kruk, M.; Jaroniec, M.; Bereznitski, Y. *J. Colloid Interface Sci.* **1996**, *182*, 282.